A COMBINED TEMPERATURE AND MAGNETIC FIELD MAPPING SYSTEM FOR SRF CAVITIES

J. Köszegi[*], B. Schmitz, K. Alomari, O. Kugeler, J. Knobloch,
Helmholtz-Zentrum Berlin, 12489 Berlin, Germany

Abstract

The commissioning results of a mapping system for a 1.3 GHz single cell cavity are presented. It combines temperature mapping with 3D magnetic field mapping along the outer surface of the resonator. It is shown that magnetic field sensors based on the anisotropic magnetoresistance (AMR) effect can be used in an SRF testing environment with improved sensitivity compared to room temperature. The system allows for the observation of dynamic effects including quench events and the normal to superconducting phase transition which impact the RF performance. A data acquisition rate of 500 Hz for all channels simultaneously (i.e., 2 ms acquisition time for a complete map) and a magnetic field resolution of currently up to 17 nT has been achieved. The details of the complete setup are presented in Reference [1].

INTRODUCTION

In the attempt to push superconducting materials for RF cavities to elevated performance, the degrading impact of trapped magnetic vortices must be investigated, understood, and ideally eliminated. Over the past years, several studies demonstrated in samples, in cavities and also in module-like operation how beneficial a reduction in trapped magnetic flux is. In particular, it was found that the level of trapped flux is impacted by numerous parameters, from cooldown conditions to material properties [2-9].

Presently, further and more systematic investigations are performed. Thus far, most of the experimental work relies on fluxgate magnetometers to measure the magnetic field during testing. The sensors measure the magnetic field component in one spatial direction and average over their length of typically 20 mm. In addition, they are costly. Therefore, previous studies applied only a limited number of sensors, often only one. Although much insight can be gained this way, an extended, systematic approach has to include effects originating from the global distribution of the magnetic field surrounding a cavity. Most notably, with a single 1D sensor it is impossible to distinguish between a change in absolute value and a change in direction of a measured magnetic field vector.

Hence, a new affordable type of sensor had to be identified which allows for high resolution magnetic field mapping at cryogenic temperatures in all three spatial directions and as a function of time. Here, we present a suitably arranged array of AMR sensors that meets the requirements. It was combined with temperature mapping [10-11] to monitor phase transitions, quench events, and local RF power dissipation during operation.
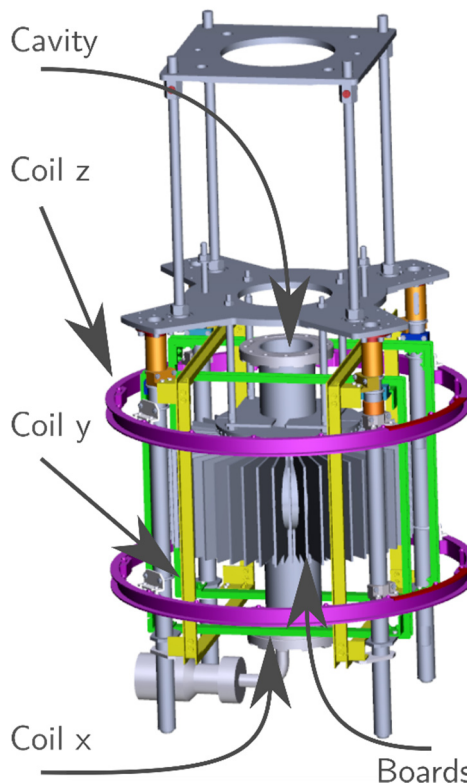
_____
* julia.koeszegi@helmholtz-berlin.de

Figure 1: Model of the cavity diagnostics system. It extends an insert of a vertical test stand and includes three pairs of Helmholtz coils as well as a brass holder with up to 48 different temperature or magnetic field measurement boards.

SYSTEM OVERVIEW

Figure 1 shows the setup of the diagnostics system mounted on a single cell TESLA type cavity. It is surrounded by three pairs of Helmholtz coils, one for each spatial direction. The temperature and magnetic field sensors are attached to printed circuit boards (PCB). The electrical supply is also realize via the PCBs which in turn are mounted to the beam pipes using a brass holder. The data of all measurement channels is acquired using IMC Spartan devices. Each device measures 128 channels with a resolution better than 10 μV using analog to digital converters and amplifier cascades. Each channel has a dedicated ADC so that multiplexing is not needed. This allows for parallel sampling of all channels with a maximum sampling rate of 500 Hz.

MAGNETIC FIELD MAPPING

AMR Technology

In most of the recent experiments on flux trapping the number of used sensors as well as the spatial resolution was limited. In the attempt to upscale to a higher resolution 3D mapping system, three goals were defined: First, overcoming the size limitation of fluxgates, second, keeping sensor-sensor interaction small, and third to keeping the system affordable.

Based on the comparison of different sensor types as presented in Reference [12], AMR sensors were chosen. They consist of four thin-film ferrite resistors arranged in a Wheatstone bridge configuration which provides sensitivity to the ambient magnetic field in one spatial direction. In comparison to the previously used fluxgate sensors, their area is approximately 0.7 mm times 0.8 mm, as opposed to a typical length of 20 mm in fluxgates. AMR sensors can exhibit a slightly better field resolution than fluxgate sensors [12]. With a cost of a few Euro each, they are significantly less expensive.

Available Sensors

Reliable AMR sensors are commercially available and produced in large quantities due to their application in mobile phones and by the automotive industry. There are several manufacturers of ready-to-use sensors. For our purposes we tested three sensors of different suppliers; the KMZ51 produced by Philips, ZMY20M produced by ZETEX and AFF755 produced by Sensitec.

As an initial test, their performance in liquid nitrogen compared to room temperature was studied [13]. The KMZ51 sensor failed operation after repeated temperature cycles and was therefore excluded from further testing. The ZMY20M and AFF755 sensors both passed. However, the AFF755 sensor showed a higher sensitivity, which was found to improve further when operated at cryogenic temperatures compared to room temperature. In addition, the AFF755 sensor includes coils for application of a test magnetic field (test-coil) and for magnetization recovery (flip-coil). Therefore, the AFF755 was chosen for further characterization and included in the mapping system. In the subsequent experiments with cavities in superfluid helium, none of the AFF755 sensors failed. Their full functionality was preserved over repeated cycles between 1.5 K and room temperature.

Magnetometry Boards

To achieve the 3D mapping, AMR sensors were positioned in groups of three facing in radial r, azimuthal φ and longitudinal z direction with respect to the cavity coordinate system. Five sensor groups were placed on one PCB. On each board, parallel connections are used for the electrical supply of the 15 sensors. The feed line is equipped with a low pass noise filter. The test-coils and the flip-coils are connected in series respectively.

Calibration

For the calibration of the sensor, the test-coil that is integrated into the AFF755 sensor can be utilized. The advantage of this approach is that no external coil is needed. Hence, the calibration can be performed even when the boards are mounted to a cavity. The test-coil is small and located close to the bridge so that neither the superconducting cavity nor the magnetic shielding impact the calibration result.

In addition, the magnetic field H generated by the test-coil only depends on the supply current I, and the geometry of the coil and can be written as

$$\mu_0 H = C \times I,$$

where C is the geometry factor of the coil which includes its length, the number of windings, and the distance to the sensor. C is assumed to be independent of temperature since thermal shrinkage was found to only have a marginal effect at the level of interest here.

The C values of the single AMRs were determined by use of a calibrated Helmholtz coil (HC) in combination with the test-coils; various HC field amplitudes were superposed with the test-coil field. Each time the test-coil current was regulated to cancel the HC field. A linear regression was performed of the HC field versus the test-coil current needed to cancel it. The slope of the regression yielded C.

We found that the C values of the various sensors showed only minor deviations and remained within a 5 percent range around the weighted mean: $C = (0.249 \pm 0.012)\ \mu T/mA$. Utilizing the determined C parameters with the test-coils, each AMR sensor can be calibrated at any given time.

The procedure including the HC described in the previous paragraphs also yields the offset voltage which originates from e.g. an asymmetry of the Wheatstone bridge, i.e. differences in the electrical resistance of the four ferrite elements. However, a calibration during operation which is only based on the C parameter cannot detect the offset voltage. Hence, at present, only changes in flux density can be measured, but absolute values at a precision on the order of 5 μT, currently cannot be determined.

Solutions for this problem of determining a change in offset during operation are currently under investigation. The results obtained with the mapping system, presented below, only show changes in magnetic field relative to a starting value which was set to zero.

COMMISSIONING RESULTS

Temperature Dependent Sensitivity

The data obtained during cold testing yielded an increase of sensitivity S at lower temperatures. S was defined as
$$V_{out} = S \times H_{applied} + V_{os}$$
where V_{out} is the output voltage of the sensor, $H_{applied}$ is a known applied magnetic field and V_{os} is the voltage offset.
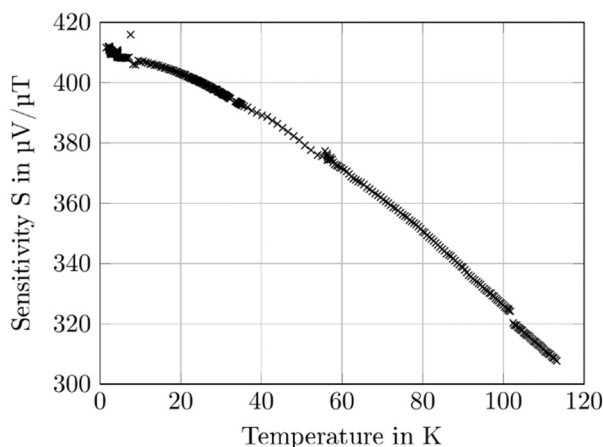
Figure 2: Measured sensitivity as a function of temperature in the range 1.5 K to 120 K. Each data point is the result of a calibration procedure.

Hence, a higher output voltage can be achieved for the same supply voltage. Figure 2 displays measured sensitivity values S of one sensor as a function of temperature T.

Since the sensitivity of each sensor changes with temperature, it also has to be calibrated individually for each operating temperature. In the test, the calibration curve was taken for all 60 sensors in use. Each sensitivity vs. temperature curve falls monotonically and looks similar to the one shown in Fig. 2. However, the absolute sensitivity at the various temperatures exhibits large differences. For 1.5 K, mean value and standard deviation of the 60 sensors was determined as $S = (330 \pm 130)\ \mu V/\mu T$. The large standard deviation makes a careful individual calibration of each sensor inevitable for reliable operation.

Flux Release During Phase Transition

The first example including an SRF cavity shows the phase transition from the superconducting to the normal conducting state. The trapped flux is measured while it is released during cavity warm-up. Since this process is slow and steady, a very smooth change in magnetic field is observed as displayed in Fig, 3. Prior to the warm up, the cavity had been cooled in $\approx 15\ \mu T$ applied field in the radial direction (on this specific board). All read-outs were zeroed at the start of the measurement since the offset was unknown. The equilibrium values towards the end of the measurement are proportional to the magnetic flux leaving at the location of the sensor. The peaks in the ΔH components are a dynamic effect of the cavity's changing magnetization as the normal conducting phase front sweeps though the cavity [14].

Flux Release During Quench

As a second example, Fig. 4 shows a combination of temperature and magnetic field measurement during a quench event. The cavity had been field-cooled in 5 µT, applied in the direction perpendicular to the board (corresponding to the azimuthal direction at the board). After the cooldown, the HC was switched off.
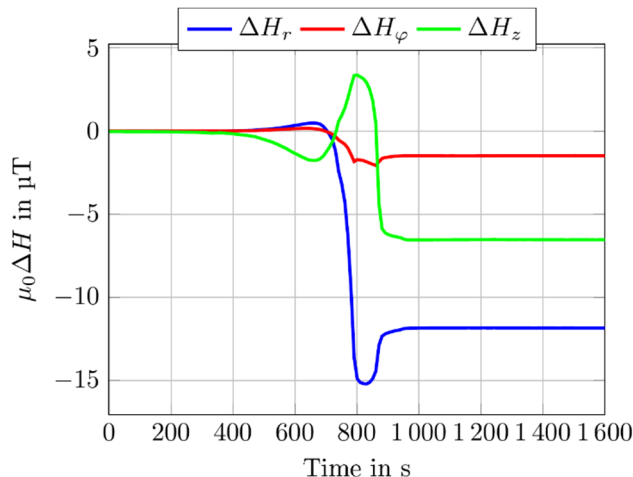

Figure 3: Release of trapped flux at the equator during warm up.

The upper graph in the figure shows the response of three temperature sensors close to the quench location at the same longitudinal position but different azimuths. The change in magnetic field measured with the magnetometry located next to the quench, as measured by the AMR in φ direction is displayed in the bottom plot. The signal was filtered for noise at 50 Hz and its higher harmonics.

The figure shows the correlation between measured temperature and magnetic field as the quench is expanding. The time between onset of the quench and full release of trapped flux is in the order of 100 ms. The dynamics of the change in magnetic field is resolved.
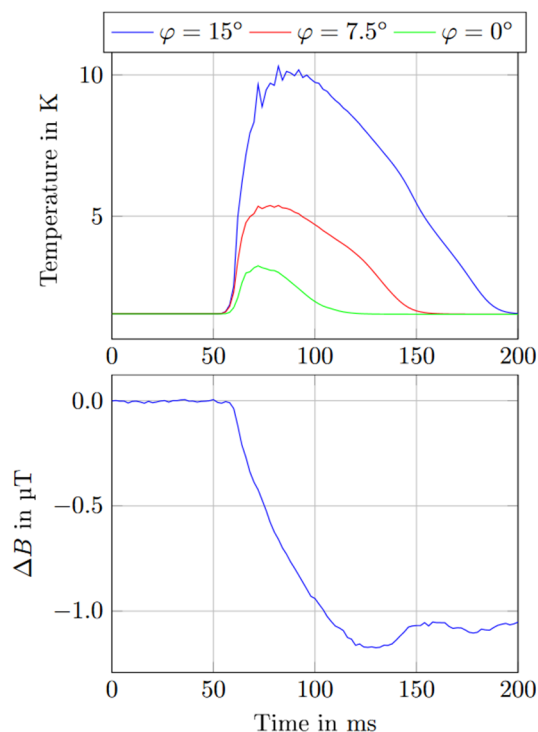

Figure 4: Combined measurement of magnetic field and temperature during a quench. Top: Response of three temperature sensors close to the quench. Bottom: AMR signal at the quench spot

REFERENCES

[1] B. Schmitz *et al.*, "Magnetometric Mapping of Superconducting RF Cavities", *Rev. Sci. Instrum.*, to be published.

[2] G. Ciovati and A. Gurevich, "Evidence of high-field radio-frequency hot spots due to trapped vortices in niobium cavities", *Phys. Rev. ST Accel. Beams*, vol. 11, p. 122001, 2008,
doi: 10.1103/PhysRevSTAB.11.122001

[3] S. Aull *et al.*, "Trapped magnetic flux in superconducting niobium samples", *Phys. Rev. ST Accel. Beams*, vol. 15, p. 062001, 2012,
doi: 10.1103/PhysRevSTAB.15.062001

[4] J.M. Vogt *et al.*, "Impact of cool-down conditions at Tc on the superconducting rf cavity quality factor", *Phys. Rev. ST Accel. Beams*, vol. 16, p. 102002, 2013,
doi: 10.1103/PhysRevSTAB.16.102002

[5] A. Romanenko *et al.*, "Ultra-high quality factors in superconducting niobium cavities in ambient magnetic fields up to 190 mG", *Appl. Phys. Lett.*, vol. 105, p. 234103, 2014, doi: 10.1063/1.4903808

[6] J.M. Vogt *et al.*, "High-Q operation of superconducting rf cavities: Potential impact of thermocurrents on the rf surface resistance", *Phys. Rev. ST Accel. Beams*, vol. 18, p. 042001, 2015,
doi: 10.1103/PhysRevSTAB.18.042001

[7] R. Eichhorn *et al.*, "Thermocurrents and their role in high Q cavity performance", *Phys. Rev. ST Accel. Beams*, vol. 19, p. 012001, 2016,
doi: 10.1103/PhysRevAccelBeams.19.012001

[8] S. Posen *et al.*, "Efficient expulsion of magnetic flux in superconducting radiofrequency cavities for high Q_0 applications", *J. Appl. Phys.*, vol. 119, p. 213903, 2016,
doi: 10.1063/1.4953087

[9] J. Köszegi *et al.*, "A magneto-optical study on magnetic flux expulsion and pinning in high-purity niobium", *J. Appl. Phys.*, vol. 122, p. 173901, 2017,
doi: 10.1063/1.4996113

[10] J. Knobloch *et al.*, "Design of a high speed, high resolution thermometry system for 1.5 GHz superconducting radio frequency cavities", *Rev. Sci. Instrum.*, vol. 65, p. 3521, 1994
doi: 10.1063/1.1144532

[11] M. Pekeler, "Thermometric study of electron emission in a 1.3 GHz superconducting cavity", Ph.D. thesis, Phys. Dept., Universität Hamburg, Hamburg, Germany, 1996.

[12] M. J. Caruso *et al.*, "A New Perspective on Magnetic Field Sensing", *Sensors (Peterborough, NH)*, vol. 15, 1998.

[13] A. L. Becker, "Charakterisierung von AMR-Sensoren bei kryogenen Temperaturen für SRF-Anwendungen", Bachelor thesis, Phys. Dept. Universität Siegen, Siegen, Germany, 2017.

[14] J. Köszegi, "Surface Resistance Minimization in SRF Cavities by Reduction of Thermocurrents and Trapped Flux", Ph.D. thesis, Phys. Dept., Universität Siegen, Siegen, Germany, 2017.